Analysis of the operation of air-cooled chillers with variable-speed fans for advanced energy-saving-oriented control strategies

Pietro Catrini, M. La Villetta, Dhirendran Munith Kumar*, Massimo Morale, Antonio Piacentino

Department of Engineering
University of Palermo, Viale delle Scienze, Palermo, Italy

Abstract

Air-cooled chillers are extensively employed to meet cooling demand in commercial and tertiary sectors. To enhance their performance during part-load operation, variable-speed drives have been integrated into compressors and condenser fans. In existing systems, condenser fans are either operated at a fixed speed or modulated to maintain a predetermined condensing pressure or temperature difference between the refrigerant and outdoor air. In the search for increased efficiency, it is worth investigating innovative control strategies aimed at minimizing energy consumption. A preliminary mapping of chiller performance at different fan speeds, loads, and operating conditions is required to achieve this goal. In this respect, this paper investigates the operation of air-cooled chillers equipped with variable-speed condenser fans, both in the case of constant- and variable-speed compressors. An ad hoc matrix test is adopted to cover appropriate ranges conditions, in terms of load and outdoor air temperatures. Performance maps are developed for a 50-kW_c chiller using a 1-D simulator. As the main findings, it may be stated that (i) in the case of the variable-speed chiller, the energy efficiency ratio increases almost linearly with fan speed, resulting in an 8.8% increase when increasing the speed from the nominal to the maximum; (ii) in the case of constant-speed chillers, the system exhibits a different behavior with the cooling capacity and the energy efficiency ratio increasing with the fan speed between 380 and 980 rpm and then decreasing (slightly or sharply, at full and part load respectively) with fan speed between 980 and 1,280 rpm, and a percentage increase of EER in the range 7.8-45% is observed. Also, the sensitivity of such results to the system design is investigated, analyzing a chiller equipped with a larger condenser that resulted in achieving minimum energy consumption at an optimal 980 rpm fan speed. Finally, for a constant-speed chiller serving an office building in the Mediterranean, the proposed fan control strategy could yield an electricity saving of up to 12.1% compared to the base case, confirming the potential for energy savings through optimized and system-tailored management of condenser fan speed.

* Corresponding author's e-mail: dhirendranmunith.kumar@unipa.it

Keywords

Air conditioning, energy savings, chillers, energy efficiency ratio, variable-speed compressor, variable-speed fans.

1. Introduction

Climate change and improved living standards for a growing share of the global population are driving an increasing need for space cooling in the world [1]. Meeting this demand sustainably necessitates not only highly efficient systems [2] but also novel approaches for generating the required energy [3]. In this regard, some authors have investigated the possibility of supplying cooling systems with heat [4] or electricity [5] directly generated onsite from renewable sources. Some researchers also investigated the concept of distributing cooling energy produced by decentralized sources through district networks [6], while others introduced innovative fault detection and diagnosis techniques to guarantee continuous performance monitoring of cooling systems [7], or developed digital twins and innovative learning algorithms for increased energy saving [8].

Air-cooled chillers stand out as a benchmark technology for addressing the cooling needs of buildings in the tertiary sector [9]. Over the last few decades, advances in the design of this technology have been implemented to ensure compliance with high-performance standards [10,11]. In addition, innovative control strategies for decreasing energy consumption have been proposed [12], the capability of implementing demand response programs in buildings through these systems has been investigated [13], and finally, innovative methods for the design of multiple-chiller systems have been developed [14]. Focusing on design improvement, manufacturers have dedicated their efforts to enhancing the efficiency of compressors when operating at part load [15]. Specifically, variable speed drives (VFD) have become increasingly prevalent in low-cooling capacity chillers, allowing for precise control of delivered cooling capacity through the modulation of compressor speed [16]. Tube and fins condensers have been gradually replaced by plate and fins condensers [17], thus leading to a reduction in refrigerant charge and the potential environmental hazards related to leakages and ineffective end-of-life fluid management [18]. New refrigerants with lower global warming potential have been developed [19]. Finally, advances have been made in the control of auxiliary systems, such as condenser fans [20], or evaporator water pumps [21].

Focusing on condenser fans, in modern small and medium chillers the rotating speed of the fan is typically modulated via VFDs, in the case of induction motors, or by using new types of electric motors such as electronically commutated motors (ECM) [22,23]. Conversely, large

chillers are typically equipped with multiple fans, and an ON-OFF control is used to sequentially switch the operation of each fan. In either case, the control aims at (i) keeping a "desired head pressure (or condensing pressure)", typically corresponding to the condensing pressure of the refrigerant calculated with the design outdoor air temperature [23] or (ii) keeping a certain "temperature difference" among the condensing refrigerant and the outdoor air (usually referred as "condensing temperature control") [24]. It is worth noting that manufacturers disclose limited information about the fan speed control strategy, considering it confidential material.

In general terms, the part-load efficiency of air-cooled chillers can be expected to improve significantly by adopting a smart control of condenser fan speed. Then, it is worth investigating whether the adoption of "optimized" setpoint values of head pressure or temperature difference would yield better performance of the unit (i.e. lower energy consumption) compared to the baseline scenario, where a constant setpoint is maintained. Meantime, these setpoint values should be also customized on the type of capacity control, *e.g.* constant-speed (loading/unloading multiple compressors to guarantee step control) or variable-speed compressor. The topic is crucial for the efficient operation of air-cooled chillers, due to the high influence of secondary fluid flow rate on the system performance [25–27]. Also, the expected behavior of the unit at lower or higher fan speeds is not easily predictable, due to the conflicting effects on (i) the energy consumption by the compressor (which decreases at higher fan speeds since the increased air flow rate lowers the head pressure of the refrigerant and the work required to move it from the evaporator to the condenser) [28] and (ii) the fan consumption, which rises with the rotating speed [26]. In principle, other factors such as the presence of dirt or dust deposits on the condenser tubes and fins would also influence the impact of fan speed on the chiller performance [29]. However, this aspect will not be discussed further in this paper.

Over the past decades, some research studies and patents have been published, specifically addressing the management strategy of variable speed condenser fans in cooling systems. In this respect, the next subsection provides an overview of these contributions.

1.1 State of art on management strategies for variable-speed condenser fans in cooling systems

Industrial research on the topic has produced some patents illustrating novel strategies aimed at pursuing specific objectives. In 2011, Singh et al. [30] proposed a logic for optimal fan speed control tailored to refrigeration systems in the food transport sector. The proposed logic was designed to minimize the power consumption of refrigeration systems by dynamically

adjusting (on an hourly basis) the setpoint of the controlled variable governing fan operation (*e.g.*, the condensing pressure or the temperature difference between the refrigerant and the outdoor air temperature). In particular, the logic monitored the energy consumption, the outdoor air temperature, and the setpoint values in each hour, adjusting the setpoint based on ad hoc indicators that result from recorded values of monitored variables in the same hour over the two preceding days. In 2014, Balistreri et al. [31] proposed a novel method for controlling variable-speed condensers in air conditioning systems. The proposed control logic aims at controlling condenser fan speed to maximize the Energy Efficiency Ratio (EER) based on refrigerant pressures measured at the compressor inlet and outlet and the condenser outlet. More specifically, while monitoring the mentioned pressures, the controller selects the condenser fan speed that maximizes the unit performance, according to "predetermined performance curves". In a recent patent by Sun and Chen [32], 2020, a control architecture for operating condenser fans in transport refrigeration systems was developed. The method considered either variable- or multi-speed fans. In the case of variable-speed fans, an optimal condensing pressure setpoint was determined based on the use of a characteristic equation of system performance with the temperature of the ambient and the refrigerant at compressor suction. Finally, the fan speed was modulated until the condensing pressure setpoint was met. In the case of a multi-speed fan, the switch from high to low speed was determined based on the actual condensing pressure and two predetermined upper and lower pressure setpoints. Finally, in 2021, Donnellan et al. [33] developed a control architecture for condenser fans in the case of refrigeration systems for the transport sector. The method set the fan speed by relying on a predetermined model of system efficiency (called by the inventors "metamodels"), developed from preliminary simulations of system operation for different operating conditions. Then, by relying on measurements by multiple sensors inserted in the refrigeration system, the controller sets the condenser fan speed which leads to the maximum performance value as predicted by the metamodel.

Moving to the scientific literature, the management of condenser fans in chillers has been investigated by a limited number of researchers. Some relevant studies were published by Yu and Chan from 2002 to 2009. Most of these published papers compared the "head pressure control" (where the condensing pressure is kept equal to the reference value at design outdoor air temperature) to the "condensing temperature control" (where the condensing temperature changes following the outdoor air temperature), extending the analysis to chillers equipped with different compressor technologies. For instance, in [34] an air-cooled chiller with a reciprocating compressor and multiple constant-speed fans was considered. Referring to an existing plant with head pressure control, a model was built and validated. Both control logics

were realized by selecting the number of fans to be staged ON and OFF. It was estimated that switching to a condensing temperature control improved the part-load performance of the chiller, with annual energy savings of up to 29%. In another study [35], the authors applied condensing temperature control for adjusting fan speed in an air-cooled chiller with screw compressors. It was estimated that the performance could increase up to 15% in the case of high outdoor temperatures and full-load operation. In [36], the authors investigated the capability of variable-speed fans to enhance the performance of chillers equipped with screw compressors. Through a validated thermodynamic model, the "head pressure" and the "condensing temperature" control strategies were again compared assuming constant- and variable-speed fans. It was found that in the case of a chiller with variable-speed fans and head pressure control, the performance change (compared to the case of constant-speed fans) was not always positive. Conversely, the adoption of a variable-speed fan together with condensing temperature control resulted in improved chiller performance under all conditions (an increase in EER up to 16% was assessed). In [37], the authors investigated the effect of variable-speed fan control in the case of an air-cooled centrifugal chiller. A control strategy based on a condensing temperature setpoint that maximized the chiller performance for each outdoor temperature value was developed. However, such a strategy required the chiller to operate at part load (around 0.7-0.84), leading to an increase in the energy consumed by the chilled water pumps. In two further studies [23,38], the authors analyzed the adoption of evaporative precooling of the air entering the condenser to enhance the performance of chillers. More specifically, in [23] the authors investigated the best strategy to vary the fans' speed in air-cooled chillers equipped with an evaporative precooler (a device made of a porous surface wetted with a film of water that evaporates in the airflow supplied to the chiller condenser). It was found that the optimal condensing temperature set point was highly dependent on the chiller load and the wet-bulb temperature of the outdoor air. The authors estimated a 5.6–113.4% increase in chiller COP, compared to a head pressure control. In [38], an air-cooled chiller equipped with mist pre-cooling at the condenser inlet was analyzed. The pre-cooling was achieved by spraying water directly on the condenser surface through nozzles, and 19.84% energy savings could be achieved by switching from head pressure to condensing temperature control.

Angermeier and Karcher [39] developed a model of an air-cooled chiller to predict the condenser fan speed which minimized the total energy consumption. The model was validated through an accurate experimental campaign, with a predicted error in performance estimation within ±10%. However, the study assumed constant evaporating pressure, compressor efficiency, subcooling, and superheating. Other studies, not strictly referring to chillers but

more generally to air-cooled refrigeration systems (in most cases, direct expansion air-conditioning units), provided further insights on management strategies for variable-speed condenser fans and are here presented for the sake of completeness. Elsayed and Kayed [40] experimentally investigated the behavior of a split air-conditioning system equipped with variable-speed compressors and variable-speed fans. The study assessed that, under steady-state conditions, an increase in the fan speed did not induce any performance improvement in the examined unit. Yeh et al. [41] proposed two control architectures for fan speed modulation (both indoor and outdoor fans) in variable-speed residential split systems, aimed at improving its energy performance and dynamic response capability. Regarding the condenser fan speed, a control strategy based on the temperature difference between the condenser and the outdoor environment was proposed. Results showed that decreasing the fan speed from 800 to 560 rpm induced a 14% decrease in the total power consumption, while the indoor temperature was only slightly affected. However, in the case of a further reduction in the fan speed to 250 rpm, an increase in total power was observed due to the higher rotating speed of the compressor. Finally, Deymi-Dashtebayaz et al. [42] developed a model to optimize the performance of a refrigeration system composed of centrifugal air-cooled chillers. The study was aimed at identifying the number of condenser fans which optimized the performance of each chiller for a given part-load ratio and outdoor air temperature. The authors estimated the potential for substantial energy savings and reduction in carbon dioxide emissions.

1.2 Scopes of the work

The above overview testifies that a limited number of studies have been devoted to analyzing the effects of condenser fan speed on air-cooled chiller performance. Most of these contributions were published more than fourteen years ago, with a majority of studies focused on air-cooled chillers with large cooling capacities (above 600 kW_c), typically equipped with screw [23,38], centrifugal [37], or reciprocating compressors [34]. There is an evident knowledge gap regarding the effects of variable-speed fans in small- to medium-scale chillers equipped with scroll compressors. Recently published papers have been predominantly focused on residential split systems [40,41]. Only a very few studies have explored the effects of fan speed management on air-cooled chillers with scrolls [39], but limited attention has been given to typical strategies employed to modulate the cooling capacity. Then, it is of paramount importance to build up scientific knowledge on this technology due to the dominant role it has been acquiring over the last decade. In addition, when addressing the topic, particular attention should be paid to the influence of the capacity control technique governing the operation of

multi-scroll chillers. Indeed, different results could be expected when sequential control is guaranteed by cycling multiple compressors alternately ON and OFF and when, conversely, continuous control is achieved by adjusting compressor speed through Variable Speed Drives to meet the demand. The provision of such information could help formulate innovative and more refined control strategies for these systems. While the problem can be stated, in general terms, as an attempt to identify optimal fan speed control strategies for air-cooled chillers equipped with scroll compressors and with different capacity control techniques, the crucial aspect lies in the need for a complete mapping of system performance in different operating conditions, aimed at detecting trade-offs between the marginal effects that any increase/decrease in fans speed induces on the power consumption by the compressors (expected to increase at lower fan speeds) and by the fan drives (expected to decrease at lower fan speeds). Also, the existence of an "optimal fan speed", capable of minimizing the total power consumption and maximizing the EER is not obvious, nor it is a priori known whether it is affected by the design specs of the unit, in terms of capacity balance among components.

To address the identified knowledge gap, this paper aims to map the behavior of an air-cooled chiller equipped with scroll compressors and variable-speed condenser fans. To cover sufficiently wide ranges for the main operation variables affecting plant operation, an ad hoc test matrix is adopted to define the complete set of required simulations. Specifically, the analyses proposed in this work are aimed at:

- Providing a comprehensive understanding of the effects of fan speed on the performance of air-cooled chillers, considering: (i) the various strategies used to modulate the cooling capacity, such as the sequential control of multiple compressors or the variable-speed control of compressors; (ii) the sensitivity of the optimal fan speed management strategy to the peculiar design features of the chiller, with a particular focus on the capacity balance between the evaporating and the condensing section of the unit (this last point will be addressed, in particular, by simulating a same system chiller when equipped with a standard and a modified condenser with increased heat transfer area).
- Covering, when performing the above analysis, a wide range of operating conditions in terms of supplied cooling capacity (thus replicating the unit behavior when facing a time-varying cooling load) and outdoor air temperature.

Regarding the examined unit, a 50-kW_c chiller equipped with constant- and variable-speed compressors is considered. Simulations are performed by a scientific 1-D tool that allows for the upload of detailed performance specs of each component drawn from commercial

catalogs. Finally, to show the potential energy saving arising from the improved ODF management, an energy analysis was carried out for the case of a constant-speed chiller serving an office building located in Palermo (Italy).

The paper is structured as follows: the second section provides details on the thermodynamic modeling of chillers in case of variable-speed fans on the condenser, and the procedure followed to develop the maps; the third section describes the reference chiller and simulated scenarios; the fourth section presents and discusses results, and the final section briefly draws conclusions.

2. Materials and Method

Before presenting in detail the procedure followed to map the operation of an air-cooled chiller with variable-speed fans, a brief description of the chiller thermodynamic modeling is due.

2.1 Thermodynamic modeling

To better understand the thermodynamic parameters and the variables considered in this work, a scheme of the chiller is presented where the main components are detailed. As shown in Fig. 1 [13], a plate heat exchanger is typically adopted as the evaporator (EVP) in air-cooled chillers. In this component, the water returning from the building at a temperature T_{wr} is cooled to the desired temperature T_{ws} and then supplied to the hydronic loop. A fan (indicated also as an "outdoor fan" or "ODF") supplies air to the condenser (CND), which can be either a tube and fins or plate and fins heat exchanger. An electronic expansion valve (EV) is used to modulate the refrigerant flow from the CND to the EVP, by controlling the refrigerant superheating at the EVP outlet. The compressor (CMP) is driven by an Induction Motor (IM), whose operation is monitored by the controller (CTRL). A detailed explanation of the controller's action was already provided by the authors in a recently published paper [13]. However, some details are here briefly repeated for the sake of self-consistency of this work. It is worth noting that in the referenced previous study [13] only the control of CMPs was assumed, not considering any optimized control for the condenser fan. Specifically, in the case of variable-speed CMPs, the referenced study assumed the controller to adjust the rotating speed of the IM until the supply temperature of cold water to the building (T_{ws}) reaches the desired setpoint. Conversely, in the case of constant-speed CMPs, the CTRL was assumed to cycle the CMPs "ON" and "OFF", by monitoring the variation of the temperature of the supplied cold water around the desired setpoint [13].

As mentioned in Section 1, ODF is typically controlled to maintain a desired value of the condensing pressure (p_{CND}) or the temperature difference between the condensing refrigerant and

the outdoor air. In the case of a variable-speed fan, the rotating speed is varied until the setpoint value is met. Conversely, in the case of a constant-speed fan, CTRL cycles the fan "ON" and "OFF" to keep the controlled variables around a desired setpoint.

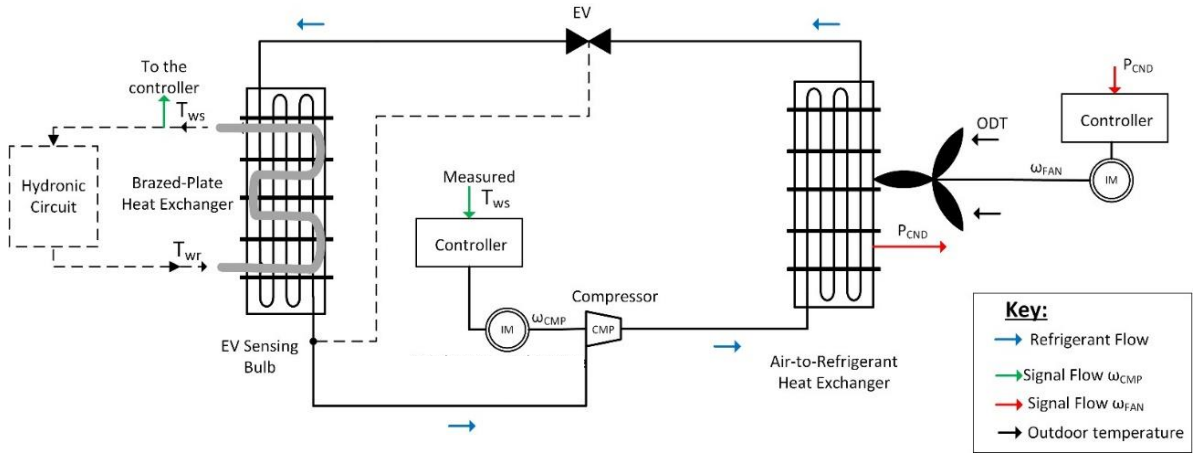

Figure 1. Components and variables of an air-cooled chiller [13].

Eqs 1.a-c shows that a convenient performance characterization of the chiller when equipped with variable-speed CMPs and variable-speed fans (briefly indicated in the following as a *variable-speed chiller*), can be achieved by expressing its cooling capacity (*CC*) and the mechanical power ($P_{m,CMP}$) absorbed by the CMPs as a function of the variables that mostly affect the performance.

$$CC = f_1(ODT, \omega_{CMP}, T_{wr}, \omega_{FAN}) \quad (1.a)$$

$$P_{m,CMP} = f_2(ODT, \omega_{CMP}, T_{wr}, \omega_{FAN}) \quad (1.b)$$

More specifically, *CC* and $P_{m,CMP}$ in variable-speed chillers are mostly dependent on the compressor's rotating speed (ω_{CMP}), the dry-bulb temperature of the outdoor air (indicated as ODT), and the temperature of the water entering the EVP (T_{wr}) [13].

Conversely, Eqs 2.a-b shows the main variables that affect the cooling capacity (*CC*) and the mechanical power ($P_{m,CMP}$) required by CMPs in the case of a chiller with constant-speed CMPs and variable-speed fans (briefly indicated in the following as a *constant-speed chiller*).

$$CC = g_1(ODT, N_{CMP}, T_{wr}, \omega_{FAN}) \quad (2.a)$$

$$P_{m,CMP} = g_2(ODT, N_{CMP}, T_{wr}, \omega_{FAN}) \quad (2.b)$$

In Eqs. 2-a.b, N_{CMP} is the number of CMPs in the state "ON". Regarding the power consumed by the fan ($P_{m,ODF}$), it essentially depends on the fan's rotating speed (ω_{FAN}) and *ODT*, as shown in Eq. 3.

$$P_{m,ODF} = h(\omega_{FAN}, ODT) \quad (3)$$

To assess the overall energy performance of the chillers, the Energy Efficiency Ratio (*EER*) is here used, as defined in Eq. 4.

$$EER = \frac{CC}{P_{m,CMP} + P_{m,ODF}} \quad (4)$$

2.2 Description of the procedure for mapping chiller operation

Fig. 2 illustrates the main steps followed to map the performance of constant-speed and variable-speed chillers equipped with variable-speed fans. According to Step no. 1, the preliminary definition of the test matrix is due, serving as a basis to identify the simulations to perform. Specifically, at this step the variation range of the variables shown in Eqs 1-2 (i.e., $ODT, T_{wr}, \omega_{CMP}$, and ω_{FAN}) is defined. In Step no. 2, the physical model of the chiller is built in ad hoc software, and simulations from the test matrix are performed. In Step no. 3, the collected data are processed by using numerical methods for developing Eqs 1.a-b and Eqs 2.a-b.

Different routes are then followed to develop maps for the constant- and variable-speed chillers. In particular, in the case of the constant-speed chiller, the EER can be easily calculated (see Step no. 4). Conversely, in the case of the variable-speed chiller, the action of the controller must be accounted for. Indeed, as previously explained, in this case, the CMP rotating speed $\omega_{CMP}$is usually modulated until the water supply temperature setpoint is met (i.e., 7 °C). It is evident that when performing a test obtained from a combination of $ODT, T_{wr}, \omega_{CMP}, \omega_{FAN}$, the resulting supply water temperature could, in general, differ from the 7 °C setpoint. For this reason, a further step is due to simulate the action of the controller. Step no. 3' describes the procedure followed for this purpose. In particular, using data available from Step no. 2, the following equation is first derived:

$$T_{ws} = f_3(ODT, T_{wr}, \omega_{CMP}, \omega_{FAN}) \quad (5)$$

Then, for a given set of $(ODT^*, T_{wr}{}^*, \omega_{FAN}^*)$ the ω_{CMP}^* value which guarantees $T_{ws} = 7\ °C$ is calculated. Once verified that the resulting ω_{CMP}^* falls within the feasible range (i.e., $\omega_{CMP,min} \leq \omega_{CMP}^* \leq \omega_{CMP,max}$, as 1000 rpm and 6200 rpm), CC and $P_{m,CMP}$ can be found.

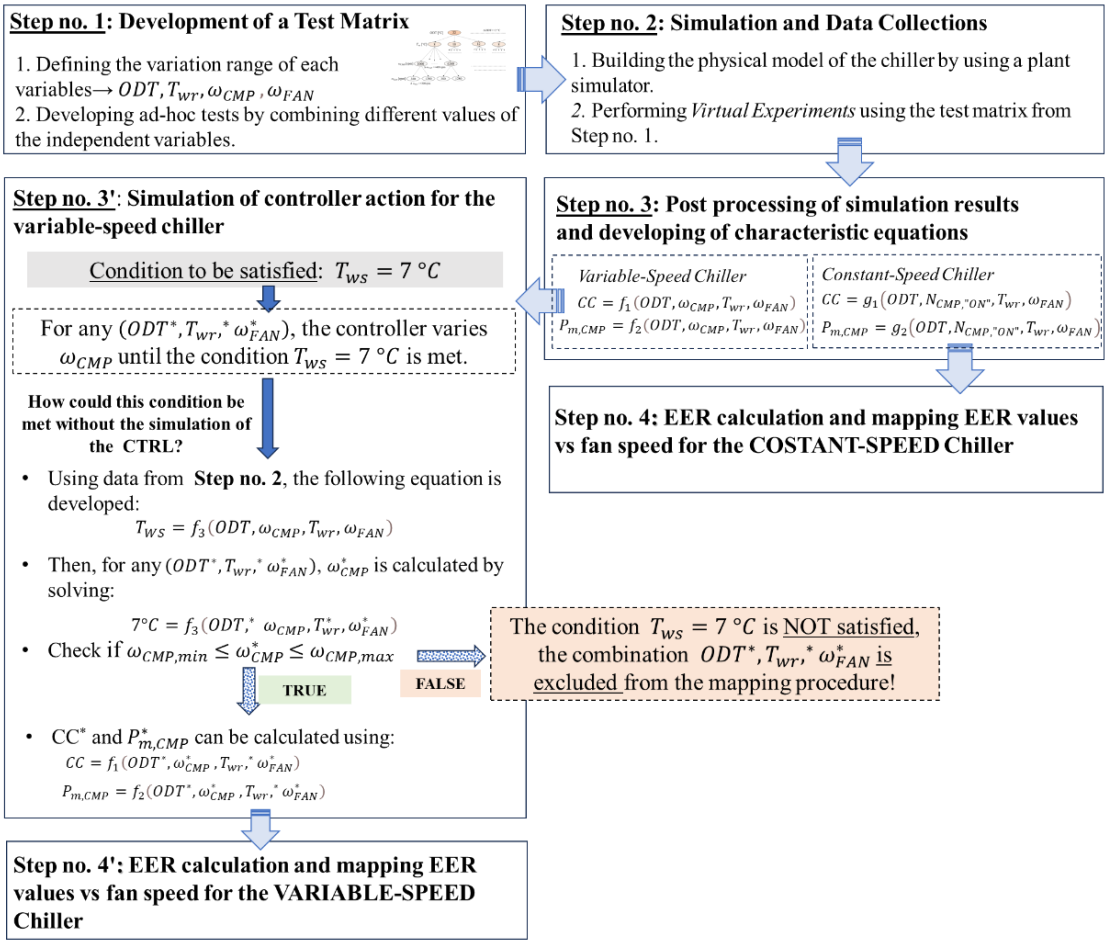

Figure 2. Scheme of the procedure followed to map the operation of the variable-speed and constant-speed chiller with variable-speed ODF.

3. Description of the reference air-cooled chiller and simulations

The nominal capacity of the reference air-cooled chiller is 49.7 kW_c (based on the rating conditions [11]: an *ODT* of 35 °C and water flow cooling from 12 °C to 7 °C). Table 1 presents the technical data of the chiller, sourced from a commercial catalog. As shown in Table 1, the unit is equipped with one axial condenser fan operating at a nominal speed of 980 rpm.

Table 1. Details of the reference air-cooled chiller [13]

Refrigerant	R410a
Condenser	Fin and Tube
Number of Condenser	1
Type of Condenser Fan	Axial
Nominal Fan Rotating Speed [rpm]	980
Condenser Fan Power [kW]	1.5
Metering Device	Electronic Expansion Valve (EEV)
Evaporator Water Flowrate [m^3/h]	7.0
Evaporator Pump Power [kW]	2
Compressor Type (and Number)	Scroll (no. 2)

Compressor Power (each) [kW]	9.0
Refrigerant Charge [kg]	14.3

As shown in Table 1, two scroll compressors are used in the reference chiller. For a more comprehensive characterization of the effect of variable-speed ODF in air-cooled chillers, two types of CMPs are here assumed:

- *variable-speed CMPs* where the speed of both CMPs varies between minimum and maximum values using VFDs until a desired supply water temperature setpoint $T_{ws,ref}$=7 °C is met.
- *constant-speed CMPs*, where the cooling demand is met by switching ON-OFF each CMP.

The above assumption on the types of compressors aligns with the current trends in commercial systems of similar capacity. Indeed, based on a survey of commercial catalogs by several manufacturers, it emerges that air-cooled chillers with nominal cooling capacity below 60 kW_c are typically equipped with variable-speed CMPs. Conversely, larger units are prevalently equipped with multiple constant-speed CMPs controlled by an 'ON-OFF' strategy. As for their applications, they are limited to small buildings as stand-alone cooling systems but they could be also found in multiple chiller layouts for medium and large buildings, in the case of either symmetric or asymmetric load sharing [14].

Regarding the ODF, the operating maps were derived by using commercial software. The curves were then transformed into a typical polynomial equation, see Eq. 6, where the ODF consumption is related to *ODT* and ω_{FAN}; coefficients have been obtained by regression, resulting in a very good agreement with the performance data declared by the manufacturer (R^2 equal to 0.99, RMSE equal to 10.38 W).

$$P_{ODF}[W] = 250.91 + 4.09\ ODT - 1.64\ \omega_{FAN} - 0.0174\ ODT^2 - 0.008\ ODT\ \omega_{FAN} + 0.0032\ \omega_{FAN}^2 \quad (6)$$

3.1 Modeling of the reference unit and description of the test matrix

The thermodynamic modeling of the reference chiller was developed via IMST-Art v. 4.0 [43]. This software performs a 1-D thermohydraulic modeling of the condenser, evaporator, and connecting lines. With regard to compressors, the tool converts the operating maps from catalogs into polynomial curves. The accuracy of results obtained via this tool has been already validated in several studies [44–47]. For the chiller investigated in the present study, data from the catalog were duly compared with the simulation results. In this regard, Fig. 3.a-b depicts

the CC and the EER for the constant-speed chiller in some operating conditions that differ in terms of *ODT* and water flow rate through the evaporator, assuming a water return temperature from the hydronic loop equal to 12 °C. The figure reveals a good agreement between simulation results and catalog data, as shown in Fig. 3.c where the percentage errors for both CC and EER are always lower than 7%, thus confirming the good accuracy of the model.

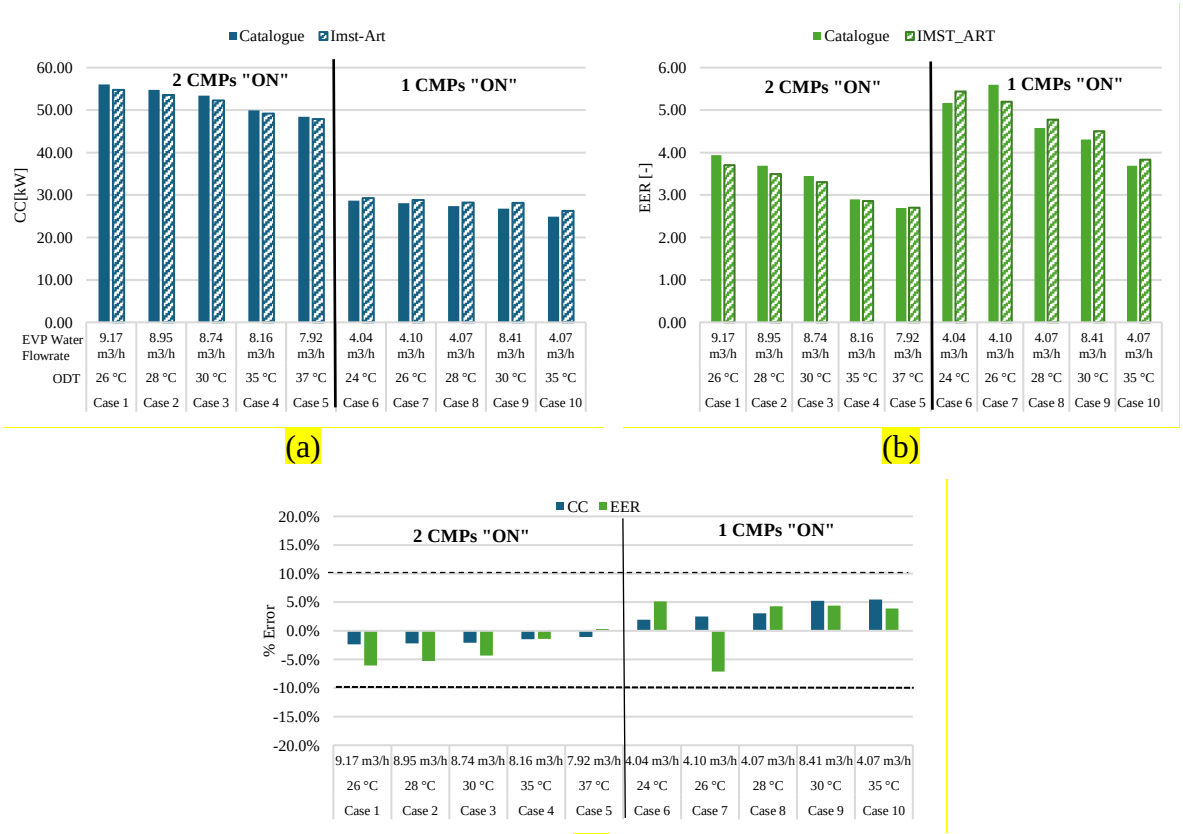

Figure 3. Comparison of IMST-Art results and data from the catalog of the chiller: (a) cooling capacity, (b) energy efficiency ratio, and (c) percentage errors.

Following the procedure in Fig. 2, the range of variation of each variable (i.e.,$ODT, T_{wr}, \omega_{CMP}, \omega_{FAN}$) was preliminary defined. The conditions to be simulated were obtained as shown in the tree diagrams in Figs 4.a-b. Regardless of the strategies adopted to operate the CMPs (see Figs 4.a-b), it was assumed that:

- *ODT* varied from 22 to 38 °C, to properly reflect different outdoor air conditions. Assuming a step variation equal to 2 °C, nine *ODT* values were simulated.
- The temperature of the water entering the EVP, T_{wr}, varied in the range of 8-12 °C to cover a wide range of cooling loads from the user. Since a variation step of 2 °C was again assumed, three values were simulated (i.e., 8 °C, 10 °C and 12 °C). As said above, the T_{wr} values are strictly related to the cooling load (since a fixed water flow rate

through the EVP is assumed): the higher the T_{wr}, the higher the cooling demand from the user. In this respect, the condition T_{wr}=12 °C reflects a maximum (i.e. 100%) cooling load condition, being the water chilled water supplied to the user at 7 °C (i.e. supply temperature setpoint) and the water flowrate set for a maximum 5 °C increase when passing through the hydronic loop of the building at maximum load condition. Such a design condition is quite common for hydronic loops supplying both fan coils or Air Handling Units (AHUs). Conversely, when T_{wr}=8 °C the cooling demand from the user is very low (only 1 °C temperature increase of the water through the hydronic loop). Under this condition, the chiller is expected to operate at part load, supplying 20% of its maximum cooling capacity.

- the ODF rotating fan varied between 380-1,280 rpm, with a step variation of 300 rpm, leading to four values to be simulated.

As shown in Fig. 4.a, in the case of the variable-speed chiller, the rotating speed of each compressor was varied between 1000 and 6200 rpm, with a variation step equal to 400 rpm (14 values to be simulated); both the CMPs are assumed to run simultaneously, in each condition, at the same ω_{FAN}. Then, by combining the *ODT* values (9) to be tested with the analogous numbers of T_{wr} (3), ω_{CMP} (14), and ω_{FAN} (4), a total of 1,512 simulations resulted to be required (see Fig. 4.a).

Regarding the constant-speed chiller, as shown in Fig. 4.b, the rotating speed of each compressor was set to 2900 rpm (i.e. the reference speed reported by catalogs). Simulations were first performed with only one CMP activated. Then, tests were repeated with two compressors "ON". Then, by combining the *ODT* values (9) to be tested with the analogous numbers of T_{wr} (3), N_{CMP}, (2), and ω_{FAN} (4), 216 simulations were performed (see Fig. 4.b).

It is worth stressing the proposed test matrix is different from the ones proposed by Standards such as ARHI 550/590 [48], as evidenced by the use of a narrower range for outdoor air dry bulb temperature (22-38°C in the present study, 12.8-52 °C in the Standard) and from the different approach adopted to consider part-load operation (here assessed in terms of instantaneous performance of the unit, rather than in average seasonal terms through indicators such as the Integral Part Load Value, IPLV, as made in Standards). The reason for adopting the proposed approach lies in the different scope of the present study (compared to Standards), not aimed at assessing performance under "rating conditions" but rather at providing a deeper understanding of condenser fans speed influence on the performance of air-cooled chillers in the most common operating conditions. The proposed approach has been already adopted by

the authors in an extensive experimental campaign [49], resulting effective in characterizing the performance of cooling systems.

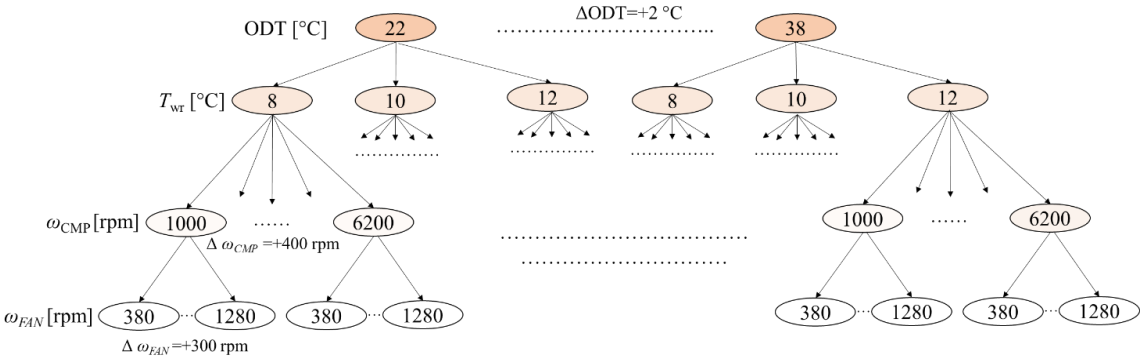

(a)

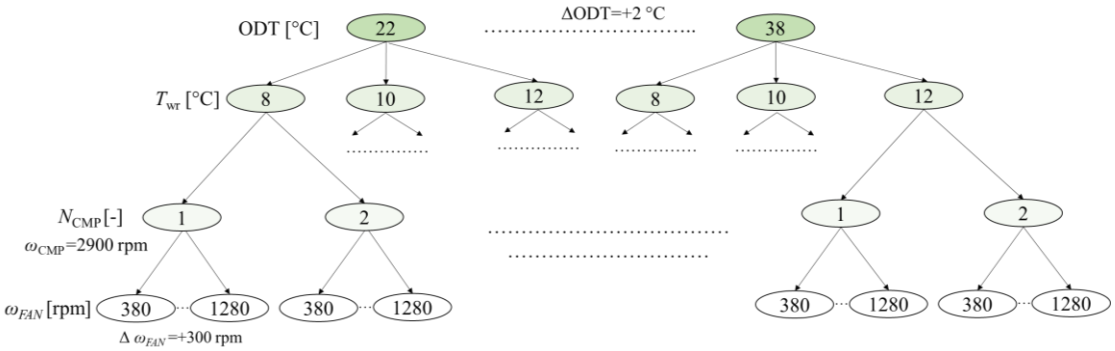

(b)

Figure 4. Tree diagram representing the test matrix for mapping the operation of (a) variable-speed and (b) constant-speed chiller with variable-speed fan on the condenser.

Data collected from simulations are then used to find Eqs 1-2 using the Least-Square (LS) technique. The resulting equations for the variable-speed chiller are detailed in Eqs 7.a,b, and for the constant-speed chiller in Eqs 8.a-b.

$$CC = 0.8684\ \omega_{CMP} - 0.2215\ ODT + 1.3211\ T_{wr} - 0.0374\ \omega_{FAN} \quad (7.a)$$

$$P_{m,CMP} = 0.0426\ \omega_{CMP} + 0.1188\ ODT - 0.4062\ T_{wr} - 0.0135\ \omega_{FAN} \quad (7.b)$$

$$CC = 17.33\ N_{CMP} - 0.21\ ODT + 1.12\ T_{wr} + 0.01\ \omega_{FAN} \quad (8.a)$$

$$P_{m,CMP} = 10.227\ N_{CMP} + 0.059\ ODT - 0.0281\ T_{wr} - 0.005\ \omega_{FAN} \quad (8.b)$$

To evaluate the error index of the proposed linear model compared to data from simulations, the Normalized Root Mean Square Error Index (NRMSE) was adopted. A good approximation was achieved by Eqs. 7-8, with an NRMSE always below 8%.

3.2 Scenario of air-cooled chillers with a "large condenser"

A further step of this analysis investigated the management of ODF in the case of a larger CND. This case could be representative of the so-called "*High Ambient*" air-cooled chiller designed for deployment in extremely hot climates, where a larger CND surface helps in reducing the condensing pressure. Consequently, the consumption of the CMPs diminishes due to the lowered condensing pressure, albeit with an increased power demand for the ODF. Indeed, a larger ODF is required to maintain an acceptable face velocity of air through the coil (e.g., 3 $m \cdot s^{-1}$). For the scope of the present study, it is worth exploring the influence of an increased size of the condenser, here assessed by assuming a 50% increase in its heat exchange area compared to the reference chiller system. This oversized condenser was designed by extending the tube length in the condenser coil of the reference unit (while guaranteeing acceptable pressure drops on the refrigerant side along the circuit). Simultaneously, the nominal air flow rate of the ODF was increased from 21,000 m^3/h to 30,000 m^3/h, with a power consumption of approximately 2,700 W at 970 rpm.

4. Results and Discussion

In this section, results for both the variable-speed and constant-speed chillers with variable-speed ODF are first presented. Then, the results for the case of a chiller with a larger condenser are shown. Finally, energy results for the case of a constant-speed chiller serving an office building are discussed.

4.1 Operation of the variable-speed chiller

The results for the variable-speed chiller with variable-speed ODF are shown in Figs 5.a-c, with reference to an *ODT* equal to 28 °C and a water return temperature from the user hydronic loop (T_{wr}) equal to 12 °C (i.e., full or 100% load condition). Fig. 5.a shows the variation of *CC* and CMP speed when the ODF speed is varied between the minimum and maximum values (i.e., 380 and 1,280 rpm). Note that regardless of the ODF speed, the CC maintains approximately constant. This result can be easily explained by considering the control logic of the variable-speed chiller. Specifically, when the ODF speed is changed, the controller adjusts the compressor speed to meet the desired chilled water temperature setpoint. Being the water flow rate and return water

temperature kept constant, whenever the unit meets the water supply temperature setpoint it operates at constant capacity. As shown in Fig. 5.a, when the ODF speed is increased, a lower condensing pressure is found due to the greater amount of air crossing the CND coil (orange line). Conversely, the evaporating pressure is almost constant (blue line). In such conditions, the decrease in the condensing pressure leads to a decrease in the quality of the refrigerant entering the EVP, eventually leading to an increased cooling effect per unit mass of circulated refrigerant. To compensate for this effect, the controller slows down the compressor (grey line) to guarantee that the water supply temperature setpoint is met.

The reduction in CMP speed leads to a reduction in the power absorbed to drive the CMP, as shown in Fig. 5.b. Meanwhile, due to the increase in the ODF speed, the ODF power consumption increases (blue line). However, the total power consumption (black line) monotonically decreases when the ODF speed increases. As shown in Fig. 5.c, the EER increases from 2.72 up to 2.96 (+8.8%) when increasing the ODF speed from 980 rpm (nominal ODF value) up to 1,280 rpm, testifying that although an increase in ODF consumption is observed (to push more air through the CND), it is more than compensated by the reduction in power consumed by the CMPs.

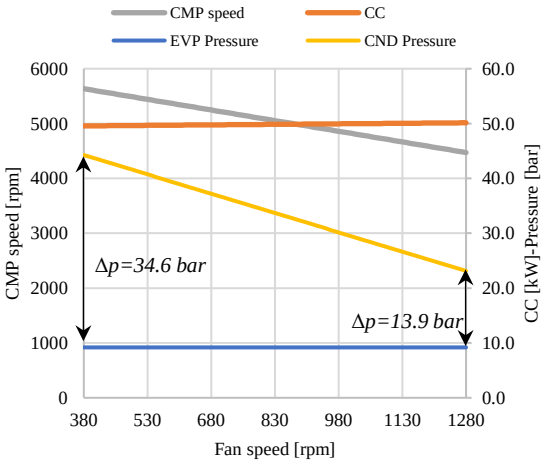

(a)

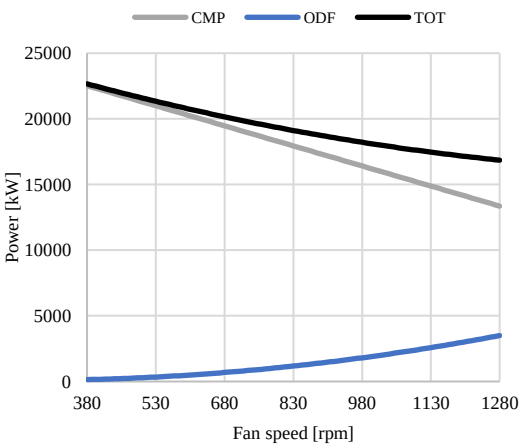

(b)

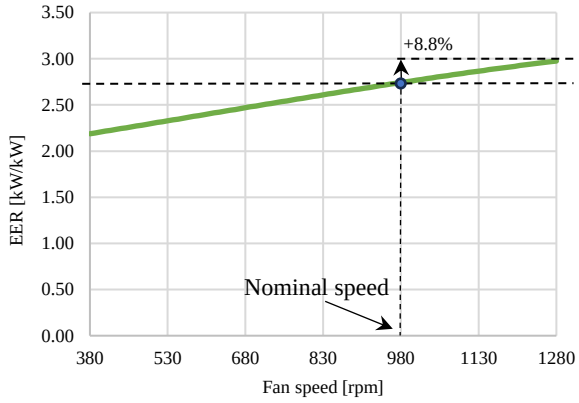

(c)

Figure 5. Results for the variable-speed chiller for *ODT*=28 °C and full-load operation: (a) Compressor speed, cooling capacity, evaporating, and condensing pressure, (b) power consumption, and (c) EER values.

Figs 6.a-b show the results for the variable-speed chiller with variable-speed ODF for the following three T_{wr} values: 12, 10.8, and 9.5 °C, again with reference to an *ODT* equal to 28 °C. As previously mentioned, T_{wr} values are strictly related to the load condition of the chiller (with higher T_{wr} values corresponding to lower cooling demand from the user). More specifically, for a T_{wr} =12 °C, the chiller is operating at full load or 100% of its capacity. Conversely, when T_{wr} =10.8 °C or T_{wr} =9.5 °C, the chiller is operating at 75% and 50% of its capacity, respectively. Note that the ODF speed was limited up to 1,000 rpm (and not to 1,280 rpm as in Fig. 5) since in the case of *ODT*=28 °C and 50% cooling load (i.e., T_{wr}=9.5 °C), higher fan velocities would lead to unfeasible operating conditions for the CMPs. More specifically, the rotating speed of CMPs would drop below 1000 rpm, which lies outside the performance map provided by the manufacturer. Looking at Fig. 6.a, results suggest that in the case of part-load operation of the chiller, it is still convenient to run the fan at its maximum speed and not to reduce it proportionally to the CMP speed. Indeed, when increasing the ODF fan speed, the decrease in CMP consumption more than offsets the increase in ODF power. In addition, when the chiller is delivering 50% of its full capacity (see grey line in Fig. 6.a), the variation of EER is heavily affected by changes in fan speed. As shown in Fig 6.b, this is motivated by the fact that at 50% part-load operation the CMP power dramatically reduces from 6.5 kW to 0.5 kW (-6.0 kW), against an increase in the ODF fan power from 0.17 kW up to 1.8 kW (+1.73 kW). In this examined scenario, reducing the ODF speed to idle (i.e., 380 rpm) would result in an EER decrease of approximately threefold compared to the value observed at 1000 rpm.

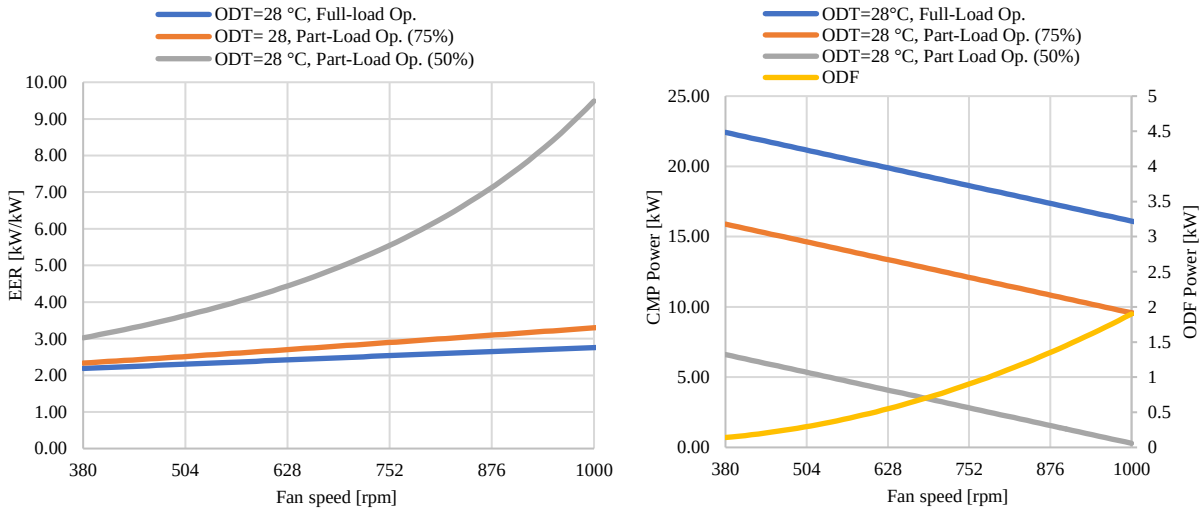

(a) (b)

Figure 6. Effects of part-load operation on the optimal CND fan speed for different *ODT* values: (a) EER values, and (b) CMP Power

Fig. 7 shows results for the variable-speed chiller's operation at three different *ODT* values (28-32 and 36°C), assuming full-load operation (i.e. T_{wr}=12 °C). A linear increase in the EER is observed when the ODF speed is increased from 380 to 1080 rpm, with a maximum percentage increase of 28.2%. In addition, a 2.9% increase is observed when moving from 980 rpm up to 1,280 rpm. This result again suggests that, regardless of the *ODT*, it is still advantageous to operate the ODF at maximum speed, as the reduction in the compressor (CMPs) power, induced by the lower difference between condensing and evaporating pressure, outweighs the increase in ODF power consumption.

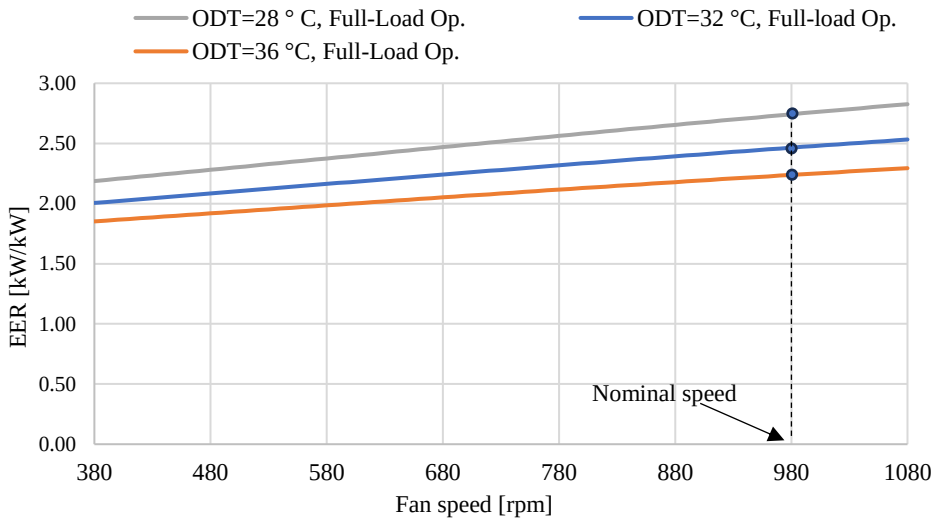

Figure 7. EER of the variable-speed chiller with variable ODF for different *ODT* values.

4.2 Operation of the constant-speed chiller

The main results for the constant-speed chillers with variable-speed ODF are presented in Figs 8.a-b for the following *ODT* values: 26, 29, 33 and 36 °C. A T_{wr} equal to 12 °C is assumed (i.e. full load condition) and both CMPs are activated. Fig. 8.a shows the variation in the *CC* when the ODF speed is varied between 380 and 1,280 rpm. Note that when the ODF speed increases from 380 to 980 rpm, the *CC* is heavily influenced by the ODF speed (a +21% increase is observed). Conversely, the sensitivity of *CC* with ODF speed reduces when passing from 980 up to 1,280 rpm (a further increase by less than 10% is observed). The sensitivity of *CC* to the fan speed is mainly related to the effects induced in the condensing pressure: indeed, as shown in Fig. 8.b, a decrease in the condensing pressure leads to a decrease in the quality of the refrigerant entering the EVP (yellow bars). Lower values of refrigerant quality lead to a higher cooling effect per kg of refrigerant circulated by the CMP. However, since the compressor speed is not modulated to meet supply temperature setpoints (differently from the case of the variable-speed chiller discussed above), the increased CC leads to a lower temperature of the water leaving the chiller and supplying the building (blue bars). As shown in Fig. 8.b, this effect is more pronounced when the ODF speed is increased from 380 rpm to 980 rpm, while it is almost negligible from 980 rpm to 1,280 rpm.

Fig. 8.c shows the total power consumed by the chillers. A minimum value is observed at 980 rpm. A further increase in the ODF speed results in an increase in total power consumption, suggesting that the increase in ODF consumption is not negligible compared to the decrease in the power needed to drive the CMP. Fig. 8.d shows the variation of EER with the ODF rotating speed. Unlike the variable-speed chiller, the EER does not monotonically increase when moving to a higher fan speed. A maximum value in the EER can be achieved at around 980 rpm (corresponding to the minimum power consumption of the unit). The percentage increase in the EER at 980 rpm is approximately equal to 45%, compared to the value observed at 380 rpm, and almost 7.8% compared to the value at 1,280 rpm.

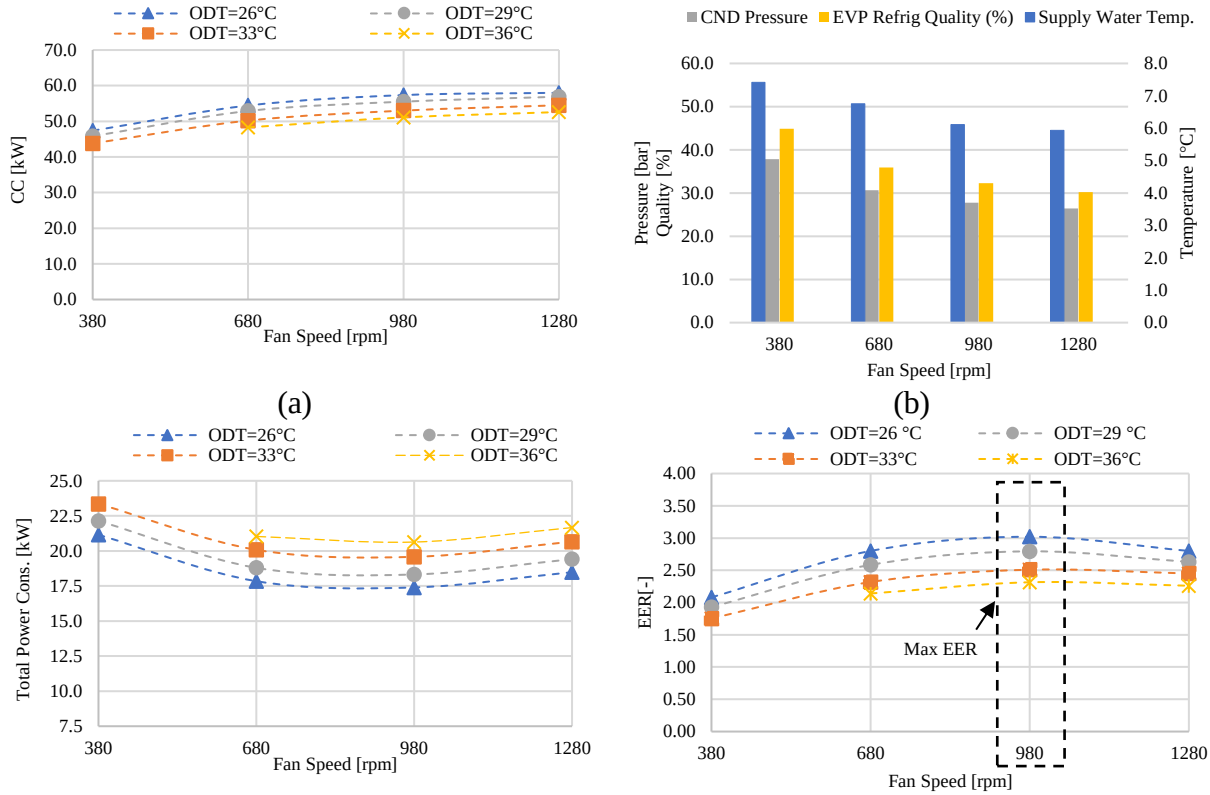

Figure 8. Results for the full-load operation of the constant-speed chiller: (a) Cooling Capacity; (b) total power consumption, (c) and (d) EER values.

The main results for the constant-speed chiller with only one CMP "ON" are shown in Figs. 9.a-b. Fig. 9.a shows the variation in the CC when the ODF speed is varied between 380 and 1,280 rpm. It may be observed that passing from 380 rpm to 980 rpm the *CC* is still influenced by the ODF speed, but the system exhibits a lower sensitivity compared to the case presented in Fig. 8.a (only a 12% increase). In addition, the *CC* is approximately insensitive to the ODF rotating speed when passing from 980 up to 1,280 rpm (a negligible 2% increase is observed). The reason for this behavior has already been explained in the case of two CMPs activated. Figure 8.b shows the variation of EER with ODF rotating speed. A maximum EER value with one CMP "ON" is achieved at around 680 rpm, i.e. at a speed lower than the optimal ODF rotating speed (i.e., 980 rpm) observed for the case of two CPMs ON. In all the cases, the percentage increase of EER when reducing the velocity from 980 to 680 rpm is almost 4.2%.

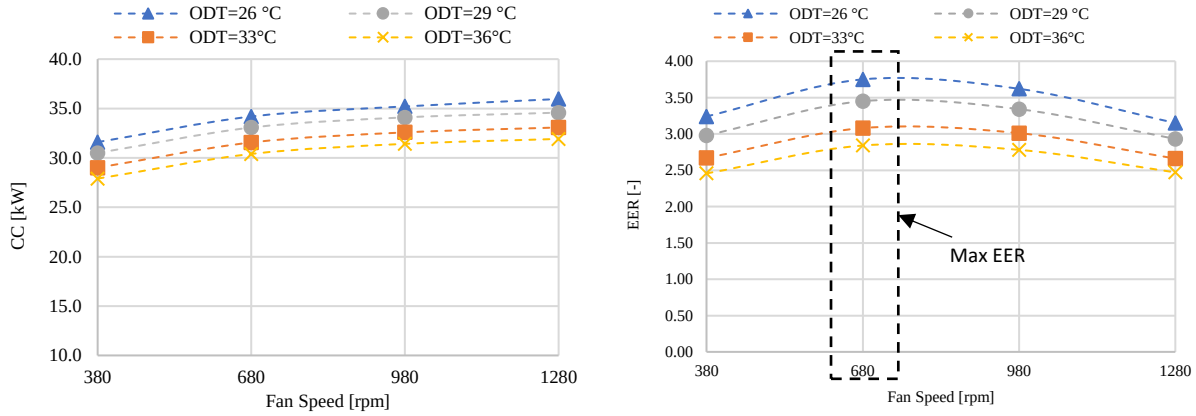

(a) (b)

Figure 9. Results for the part-load operation of the constant-speed chiller (i.e., one compressor "ON"): (a) Cooling Capacity, and (b) EER values.

4.3 Effects of condenser size on the optimal fan speed

Figs 10.a shows the EER values for the variable-speed chiller equipped with variable-speed ODF, in the case of the chiller with a larger CND as discussed in Section 3.2. The following three T_{wr} values were assumed: 12, 10.8, and 9.5 °C, corresponding to 100%-, 75%-, and 50%-part load conditions, respectively. It can be observed that the EER no longer exhibits the monotonically increasing trend at higher fan speeds observed in Fig. 5.c for the unit equipped with a smaller condenser; conversely, an optimal ODF speed lower than the maximum 1,280 rpm can be identified. The existence of such a maximum EER can be explained by looking at Fig. 10.b where, for the simulation performed at *ODT*=28 °C and 50% part-load, the same rotating speed corresponds to the minimum value of the total power consumption of the chiller. In addition, as shown in Fig. 10.a, regardless of the examined loading condition (100%, 75%, and 50% cooling demand from the user), the maximum value of EER maintains approximately constant at the same ODF fan speed. Finally, the effect of different *ODT* values is shown in Fig. 10.c. Interestingly, no sensitivity in the optimal ODF speed to changes in *ODT* is observed.

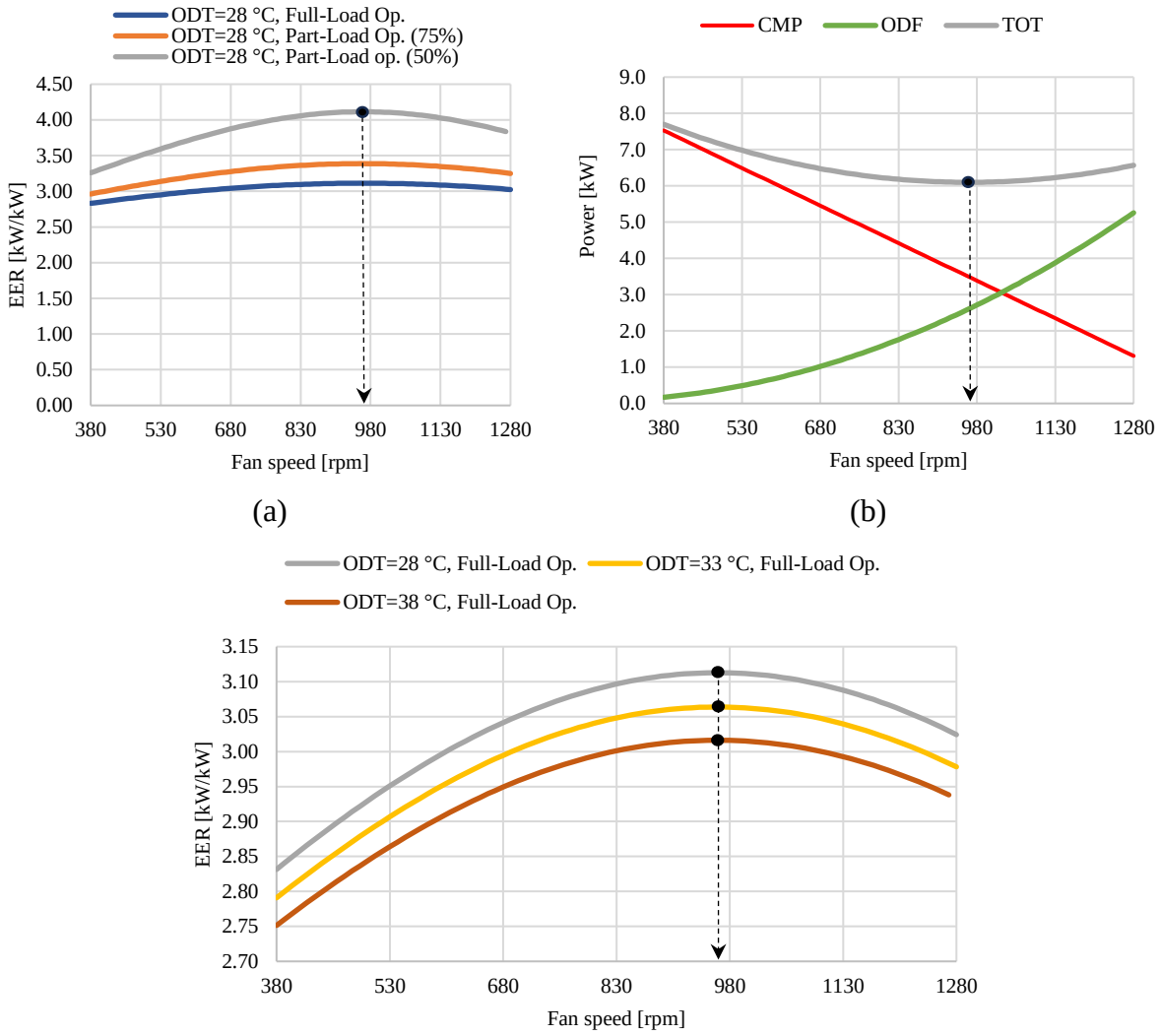

Figure 10. (a) EER values and (b) power consumption for the variable-speed chiller with a "large condenser" at full load.

Figs 11.a,b show the EER trend for the same unit, equipped with the larger condenser, in the case of the constant-speed capacity control. Looking at Fig. 10.a, when both the CMPs are running (i.e., at full capacity), a maximum EER value is achieved in the middle of the range 680-980 rpm. As already explained in Subsection 4.2, the existence of such a maximum is related to the change in the CC and the decrease in CMP power, induced by the increase in the airflow rate through the CND coil. When running only one CMP (see Fig. 11.b) the maximum EER value is located at 680 rpm. Furthermore, a strong reduction in the EER is observed when passing from 680 rpm to 1,280 rpm (i.e. -45%). This result is a consequence of the lower sensitivity of the CC in this range, and the increase in ODF power consumption as observed in Fig. 8.b.

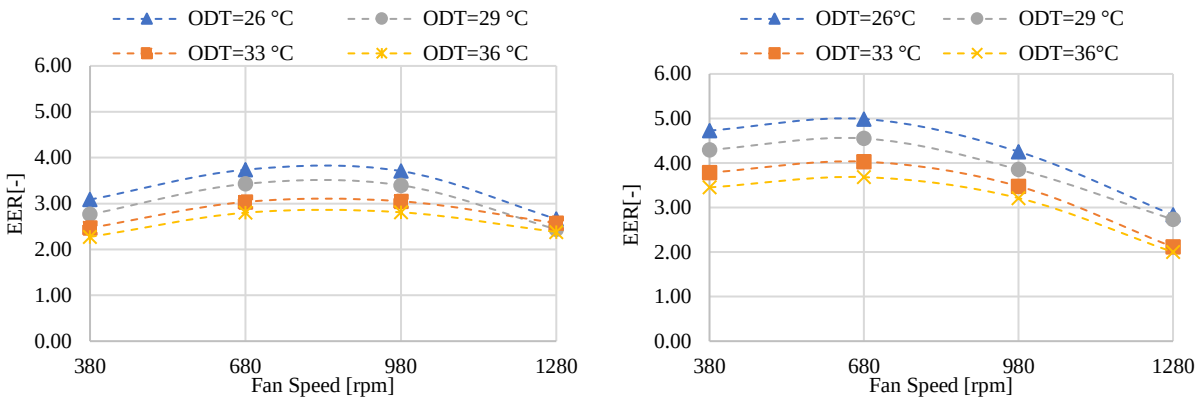

Figure 11. EER values for the constant-speed chiller with a "large condenser": (a) full load operation (two CMPs ON) and (b) 50% part-load operation (only one CMPs ON)

4.4 On the relevance of appropriate speed control strategies for variable-speed fans in air-cooled chillers

Before moving on, it is essential to summarize the key findings that emerged in the previous sections with regard to air-cooled chillers with variable-speed ODFs. In both variable-speed and constant-speed chillers, the results indicated that a significant potential for energy savings through effective ODF control exists. Specifically, in variable-speed chillers, allowing the ODF to operate at maximum speed, rather than relying on constant-speed ODFs, could be advantageous. Interestingly, a simplified control method that sets the ODF speed proportionally to the compressor speed may not result in energy savings, particularly during part-load operations. Conversely, in constant-speed chillers, an optimal ODF speed value may exist, mainly depending on the number of activated compressors rather than on the outdoor air temperature. Interestingly, in this case, a simplistic approach that sets the condenser fan to maximum speed when two compressors are activated or to minimum speed when only one is active may not lead to energy savings.

Finally, it is crucial to emphasize that the above-formulated criteria must be validated by considering the technical specifications of the chiller, including heat exchanger and compressor types. Therefore, a preliminary assessment through proper mapping of the chiller's performance is necessary.

4.5 Assessment of the energy-saving potential of the improved fan management strategy

In order to assess the potential energy saving arising from the improved ODF management, an analysis was carried out for the case of the examined constant-speed chiller when serving an office building located in Palermo (Italy). The main features of the assumed building (geometry, envelope, and so on) are standardized according to ASHRAE 90.1-2016 [50] and adapted to Italian building stock by using the UNI/TR 11552:2014 [51]. The building was simulated in TRaNsient

SYstem Simulation software [52]. The obtained cooling demand is shown in Fig. 12, and it spans from June 1st to September 30th. The profile was obtained considering (i) schedules for occupants, equipment, and lightning according to [50], and (ii) local control of the indoor air temperature, maintained at approximately 26 °C. A peak cooling demand of about 49 kW_c was found. *ODT* values for Palermo, which are shown in Fig. 11, were retrieved from Meteonorm Database [53].

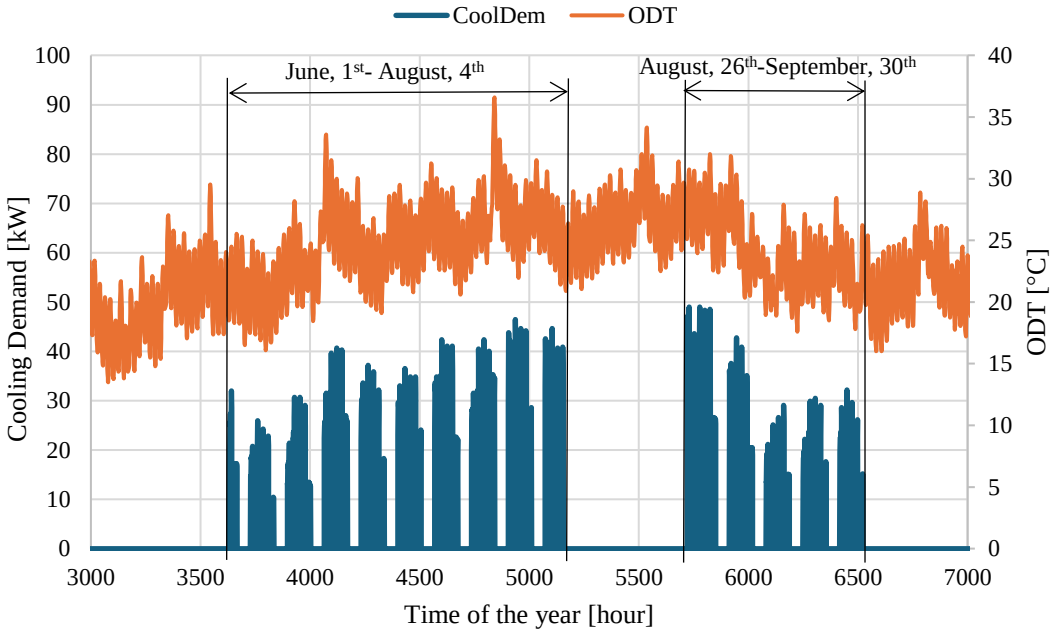

Figure 12. Cooling demand profile of the office building.

The constant-speed chiller previously examined was assumed to meet the cooling demand of the office. The chiller was connected to a cold thermal storage system of about 1 m^3 volume. Moreover, a sequential control was assumed to switch ON and OFF chiller compressors based on the temperature measured at the bottom node of the tank [13]. More specifically, a temperature setpoint of 7 °C for the supply water was assumed, with a maximum deadband of ± 2 °C. Regarding the ODF, the following scenarios were considered:

- *Base case.* A head pressure control for managing the ODF of the chiller (here indicated as HP) was assumed as a base case. More specifically, it was assumed to maintain a pressure of about 28.5 bar corresponding to an average saturation temperature of 45 °C for R410a. To simulate such a logic, maps for the chiller were developed similarly to the procedure shown in Fig. 2. However, for the sake of brevity, the procedure is not described.
- *Improved Scenario.* It was assumed to set the fan speed so that the maximum EER value (shown in Figs. 8 and 9) is achieved. More specifically, the ODF rotating speed was set

to 980 rpm in the case two CMPs are activated, and 680 rpm in the case only one compressor is ON.

4.5.1 Definition of the indicators and results

To compare the energy performance of the two control logics, an average EER value was defined as shown in Eq. 9. More specifically, $\overline{EER}^{[\alpha\%:\beta\%]}_{[ODT_1;ODT_2]}$ in the equation indicates the average EER of the chiller when operated at a percentage of its full capacity lying in the $[\alpha\%:\beta\%]$ range, with an *ODT* within the interval [ODT_1, ODT_2].

$$\overline{EER}^{[\alpha\%:\beta\%]}_{[ODT_1;ODT_2]} = \frac{\sum_{i=1}^{8760} CoolDem_{i,[ODT_1;ODT_2]} EER^{[x\%]}_{ODT_i}}{CoolDem_{[ODT_1;ODT_2]}} \quad (9)$$

In Eq. 9 $CoolDem_{[ODT_1;ODT_2]}$ indicates the total cumulated cooling energy demanded by the building, throughout the heating season, when *ODT* lies in the range between ODT_1 and ODT_2. $CoolDem_{i,[ODT_1;ODT_2]}$ denotes, conversely, the cooling demand in a generic *i*-th hour, while $EER^{[x\%]}_{ODT_i}$ is the EER calculated in the *i*-th hour with the chiller operating at x% of its full capacity (with x% falling in $[\alpha\%:\beta\%]$). The following temperature intervals were assumed to develop a frequency distribution of the hourly cooling load resulting from TRNSYS simulations: [23-25 °C], [25-28 °C], [29-31 °C], [32-34 °C], and [35-37 °C]. Considering that the chiller is equipped with two compressors the following part-load ranges were assumed: [0-50%] and [50%-100%].

Results are shown in Fig. 13. The pink bars represent the percentage of the annual cooling energy demanded in each ODT range [ODT_1-ODT_2], which is met by operating the chiller at a certain part-load ratio. As intuitive, at higher ODT (see last three intervals), the cooling load from the building is very high and, based on the capacity control assumed, the entire load would be supplied by the unit when running with two compressors "ON"; conversely, at lower ODT values a significant fraction of the cooling energy would be supplied with the unit in part-load operation and one compressor only in "ON" state.

Looking at the green markers indicating the EER values achieved by the chillers at different ODT and loading conditions, it is worth noting that the EER of the chiller operating with the improved ODF speed control strategy (indicated as Var_ODF) outperforms the chiller with HP control in the case of low and medium *ODT* values (i.e., for ODT ranging between 23 and 28 °C). Conversely, the increase in the EER is much lower when moving to higher *ODT* values. For instance, in the ranges [29-31°C] and [32-34 °C], the percentage increase of the average EER in the case of Var_ODF is approximately equal to 4.5% and 6.5%, respectively. In the range [35-37 °C] the HP control even outperforms the Var_ODF control, since at such highest outdoor air

temperatures the higher ODF speed adopted in the HP control results in a lower condensing pressure. Finally, considering the total electricity consumption in one year of operation and based on the average EER defined by Eq. 9, it was found that the Var_ODF control resulted in 3.79 MWh_e/y, while the HP control to 4.31 MWh_e/y. Then, the improved ODF speed control strategy identified in Section 4.2 resulted in a marginal 12.1% energy saving compared to the conventional control strategy adopted as a reference case.

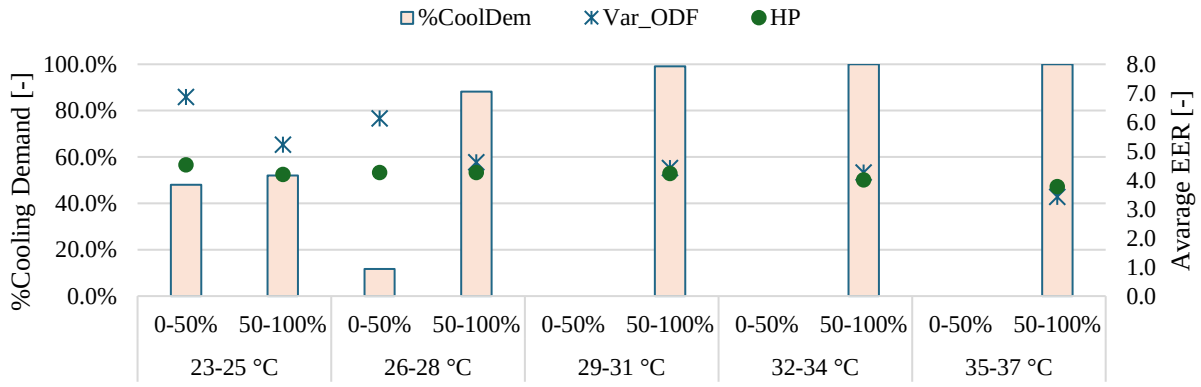

Figure 13. Average EER values for the two management strategies.

5. Conclusions

In this paper, the performance of air-cooled chillers equipped with variable-speed condenser fans was investigated, to identify optimal control strategies of fan speed. By assuming a 50-kWc chiller as a reference unit, a complete mapping of system performance was obtained through several simulations performed in a wide set of operating conditions (collected in a test matrix), specified in terms of outdoor temperature and cooling load (this last term imposed by fixing different return temperature of the water on the hydronic loop), considering both the cases of the unit equipped with constant- and variable-speed compressors. Simulation results were collected in terms of power absorption by compressors and fans' drives and EER of the unit. In the case of the chiller with variable-speed compressors, the EER increased by about 8.8% when increasing the fan speed with respect to the nominal speed value. Due to this monotonic trend, in such a configuration keeping the fans at the highest speed is convenient. In the case of the constant-speed chiller, when operating at full load (i.e. both compressors activated), the cooling capacity is very sensitive to the outdoor fan speed, increasing by 21% when the fan rotating speed increased from 380 rpm to 980 rpm, for higher fans speed, from 980 up to 1,280 rpm, the capacity resulted approximately constant (actually, a 1% decrease was observed). Therefore, unlike the variable-speed chiller, in units equipped with sequential control of multiple constant-speed compressors the

EER no longer exhibits a monotonic trend, rather achieving a maximum value corresponding to a particular fan speed (980 rpm for the examined unit, coincident with the nominal rotating speed of the fan), which should be identified as "optimal fans rotating speed" for the examined conditions. When simulating the part-load operation of the same unit (only one of the two compressors activated), the maximum EER was achieved at a lower fan rotating speed, around 680 rpm. An optimal condenser fan control of the unit should consequently reduce the rotating speed whenever the unit reduces the load. The effect of condenser fan speed on the same variable-speed chiller when supposed equipped with a larger condenser was investigated, resulting in a very different trend from the one observed for the "base design": the unit with a larger condenser achieved a maximum EER for a particular fan speed. The discrepancy between the results obtained for the units with a "base design" and with an "increased size condenser" testifies that no rules of general validity can be drawn for the optimal control of condenser fan speed since the energetically optimal strategy is highly influenced by the capacity balance between components and should be therefore identified for each unit through an accurate performance map under different operating conditions. Finally, in the case of a constant-speed chiller serving an office building, the application of the improved strategy for fan control revealed that potential for energy savings exists compared to conventional logic based on a fixed setpoint on condensing pressure, resulting in a 12.1% reduction in electricity consumption. The study confirms that an in-depth assessment of system performance aimed at identifying optimal control of auxiliaries is worth investigating since relevant margins for energy savings exist especially for systems with prolonged annual operation in off-rating and part-load conditions. In broader terms, improving the performance of these systems is of utmost importance considering the expected increase in building cooling demand due to global warming. In this regard, as air-cooled chillers will be reference technologies primarily because of their simplicity, a decrease in the energy required during their operational phase through refined controls will contribute to the achievement of ambitious decarbonization goals. Future work will focus on controlling the building architecture in the case of variable-speed fan chillers, including the maps developed here to estimate the energy-saving potential of different buildings in the tertiary sector.

Acknowledgment

This study was developed in the framework of the research activities carried out within the PRIN 2020 project: "OPTIMISM—Optimal refurbishment design and management of small energy micro-grids", funded by the Italian Ministry of University and Research (MUR).

Declaration of author statement

Pietro Catrini: Conceptualization, methodology, software, validation, investigation, data curation, writing-original draft preparation, visualization. **Maurizio La Villetta:** Conceptualization, methodology, software, validation, investigation, data curation, writing-original draft preparation, visualization. **Dhirendran Munith Kumar:** data curation, writing-original draft preparation, visualization**. Massimo Morale:** Conceptualization. **Antonio Piacentino:** Conceptualization, writing—review and editing, supervision.

Nomenclature

Acronyms

CMP	Compressor
CND	Condenser
CTRL	Control
ECM	Electronically Commutated Motor
EVP	Evaporator
EV	Expansion Valve
IM	Induction Motor
LS	Least Square
ODF	Outdoor Fan
VFD	Variable frequency drive

Variables

CC	Cooling Capacity (W)
CoolDem	Cooling Demand(W)
EER	Energy Efficiency Ratio (dimensionless)
P_{m}	Mechanical Power (W)
RMSE	Root Mean Square Error Index
ODT	Outdoor air temperature (°C)
$T_{\mathrm{ws,ref}}$	Reference Temperature of the water supplied to the hydronic loop (°C)
T_{wr}	Temperature of the water returning from the hydronic loop (°C)
T_{ws}	Temperature of the water supplied to the hydronic loop (°C)

Greek Letters

ω_{CMP}	Compressor rotating speed (rpm)
ω_{FAN}	Fan rotating speed (rpm)

References

[1] Pezzutto S, Quaglini G, Riviere P, Kranzl L, Novelli A, Zambito A, et al. Screening of Cooling Technologies in Europe: Alternatives to Vapour Compression and Possible Market Developments. Sustainability 2022;14:2971. https://doi.org/10.3390/su14052971.

[2] International Energy Agency (IEA). Space Cooling. 2022. Available at: https://www.iea.org/reports/space-cooling-2

[3] Calise F, Liberato Cappiello F, Cimmino L, Dentice d'Accadia M, Vicidomini M. Optimal design of a 5th generation district heating and cooling network based on seawater heat pumps. Energy Convers Manag 2022;267:115912. https://doi.org/10.1016/j.enconman.2022.115912.

[4] Alahmer A, Ajib S. Solar cooling technologies: State of art and perspectives. Energy Convers Manag 2020;214:112896. https://doi.org/10.1016/j.enconman.2020.112896.
[5] Calise F, Figaj R.D, Vanoli L. A novel polygeneration system integrating photovoltaic/thermal collectors, solar assisted heat pump, adsorption chiller and electrical energy storage: Dynamic and energy-economic analysis. Energy Convers Manag 2017;149:798–814. https://doi.org/10.1016/j.enconman.2017.03.027.
[6] Bilardo M, Sandrone F, Zanzottera G, Fabrizio E. Modelling a fifth-generation bidirectional low temperature district heating and cooling (5GDHC) network for nearly Zero Energy District (nZED). Energy Reports 2021;7:8390–405. https://doi.org/10.1016/j.egyr.2021.04.054.
[7] Barandier P, Marques Cardoso A.J. A review of fault diagnostics in heat pumps systems. Appl Therm Eng 2023;228:120454. https://doi.org/10.1016/J.APPLTHERMALENG.2023.120454.
[8] Chen K, Zhu X, Anduv B, Jin X, Du Z. Digital twins model and its updating method for heating, ventilation and air conditioning system using broad learning system algorithm. Energy 2022;251:124040. https://doi.org/10.1016/j.energy.2022.124040.
[9] Elnagar E, Pezzutto S, Duplessis B, Fontenaille T, Lemort V. A comprehensive scouting of space cooling technologies in Europe: Key characteristics and development trends. Renewable and Sustainable Energy Reviews 2023;186:113636. https://doi.org/10.1016/J.RSER.2023.113636.
[10] European Standards. EN 14825:2022-Air conditioners, liquid chilling packages and heat pumps, with electrically driven compressors, for space heating and cooling, commercial and process cooling 2022.
[11] European Standards. EN 14511:2022-Air conditioners, liquid chilling packages and heat pumps for space heating and cooling and process chillers, with electrically driven compressors. 2022.
[12] Bechtel S, Rafii-Tabrizi S, Scholzen F, Hadji-Minaglou J-R, Maas S. Influence of thermal energy storage and heat pump parametrization for demand-side-management in a nearly-zero-energy-building using model predictive control. Energy Build 2020;226:110364. https://doi.org/10.1016/j.enbuild.2020.110364.
[13] Kumar D.M, Catrini P, Piacentino A, Cirrincione M. Advanced modeling and energy-saving-oriented assessment of control strategies for air-cooled chillers in space cooling applications. Energy Convers Manag 2023;291:117258. https://doi.org/10.1016/j.enconman.2023.117258.
[14] Catrini P, Piacentino A, Cardona F, Ciulla G. Exergoeconomic analysis as support in decision-making for the design and operation of multiple chiller systems in air conditioning applications. Energy Convers Manag 2020;220:113051. https://doi.org/10.1016/j.enconman.2020.113051.
[15] Cai J, Braun J.E. Assessments of variable-speed equipment for packaged rooftop units (RTUs) in the United States. Energy Build 2018;164:203–18. https://doi.org/10.1016/j.enbuild.2018.01.007.
[16] Kouropoulos G.P. Review of the Capacity Control Capability of Commercial Air Conditioner Units with Variable Speed Compressor. International Journal of Air-Conditioning and Refrigeration 2016;24:1630005. https://doi.org/10.1142/S2010132516300056.
[17] Bell I.H, Groll E.A. Air-side particulate fouling of microchannel heat exchangers: Experimental comparison of air-side pressure drop and heat transfer with plate-fin heat exchanger. Appl Therm Eng 2011;31:742–9. https://doi.org/10.1016/j.applthermaleng.2010.10.019.

[18] Paurine A, Maidment G.G, Rodway M, Yebiyo M. Understanding the market need for skills in alternative refrigerants with low global warming potential in the EU region – A comprehensive survey on Refrigerant Emissions And Leakage (REAL) alternatives programme. International Journal of Refrigeration 2021;122:11–20. https://doi.org/10.1016/j.ijrefrig.2020.11.014.
[19] Nair V. HFO refrigerants: A review of present status and future prospects. International Journal of Refrigeration 2021;122:156–70. https://doi.org/10.1016/j.ijrefrig.2020.10.039.
[20] Yanik M. Is variable fan speed an answer to part-load efficiency in modular aircooled chillers and heat pumps. Danfoss 2018.
[21] Trautman N, Razban A, Chen J. Overall chilled water system energy consumption modeling and optimization. Appl Energy 2021;299:117166. https://doi.org/10.1016/J.APENERGY.2021.117166.
[22] Tirmizi S.A, Gandhidasan P, Zubair SM. Performance analysis of a chilled water system with various pumping schemes. Appl Energy 2012;100:238–48. https://doi.org/10.1016/j.apenergy.2012.05.052.
[23] Yu F.W, Chan K.T. Improved condenser design and condenser-fan operation for air-cooled chillers. Appl Energy 2006;83:628–48. https://doi.org/10.1016/j.apenergy.2005.05.007.
[24] Schneider Electric. Dynamic Speed Modulation of Condenser Fans in Chiller Systems. Schneider Electric 2010.
[25] Yu F.W, Chan K.T. Optimization of water-cooled chiller system with load-based speed control. Appl Energy 2008;85:931–50. https://doi.org/10.1016/J.APENERGY.2008.02.008.
[26] Sezen K. Influence of airflow rates on air source heat pump operating parameters. Appl Therm Eng 2023;233:121123. https://doi.org/10.1016/j.applthermaleng.2023.121123.
[27] Amr Owes Elsayed. Management of Condenser Fan Speed and its Influence on the Split Air Conditioner Performance. Global Journal of Energy Technology Research Updates 2019;6:41–8. https://doi.org/10.15377/2409-5818.2019.06.4.
[28] Li H, Braun J.E. Decoupling features and virtual sensors for diagnosis of faults in vapor compression air conditioners. International Journal of Refrigeration 2007;30:546–64. https://doi.org/10.1016/j.ijrefrig.2006.07.024.
[29] Pelella F, Viscito L, Mauro A.W. Combined effects of refrigerant leakages and fouling on air-source heat pump performances in cooling mode. Appl Therm Eng 2022;204:117965. https://doi.org/10.1016/j.applthermaleng.2021.117965.
[30] Singh A, Mathews T.J, Brown F.C, Ozgur Y.G. Condenser Fan Control System. US 8,051,668 B2, 2011.
[31] Balistreri M, D. Daddis E, Nieva K.J. Condenser fan speed control for air conditioning system efficiency optimization. US 2014/0140810 A1, 2014.
[32] Sun J, Chen L. Refrigeration System Condenser Fan Control. US 10,697,683 B, 2020.
[33] Donnellan W, Premchand RP, Greene M, Conde JE. Speed control strategies for a condenser fan in a refrigeration system. US 2021/0278115 A1, 2021.
[34] Chan K.T, Yu F.W. Applying condensing-temperature control in air-cooled reciprocating water chillers for energy efficiency. Appl Energy 2002;72:565–81. https://doi.org/10.1016/S0306-2619(02)00053-3.
[35] Chan K.T, Yu F.W. Thermodynamic-behaviour model for air-cooled screw chillers with a variable set-point condensing temperature. Appl Energy 2006;83:265–79. https://doi.org/10.1016/J.APENERGY.2005.01.009.

[36] Yu F.W, Chan K.T. Modelling of the coefficient of performance of an air-cooled screw chiller with variable speed condenser fans. Build Environ 2006;41:407–17. https://doi.org/10.1016/j.buildenv.2005.02.002.
[37] Yu F.W, Chan K.T. Part load performance of air-cooled centrifugal chillers with variable speed condenser fan control. Build Environ 2007;42:3816–29. https://doi.org/10.1016/j.buildenv.2006.11.029.
[38] Yu F.W, Chan K.T. Simulation and electricity savings estimation of air-cooled centrifugal chiller system with mist pre-cooling. Appl Energy 2010;87:1198–206. https://doi.org/10.1016/J.APENERGY.2009.08.023.
[39] Angermeier S, Karcher C. Model-Based Condenser Fan Speed Optimization of Vapor Compression Systems. Energies 2020;13:6012. https://doi.org/10.3390/en13226012.
[40] Elsayed A.O, Kayed T.S. Dynamic performance analysis of inverter-driven split air conditioner. International Journal of Refrigeration 2020;118:443–52. https://doi.org/10.1016/J.IJREFRIG.2020.05.014.
[41] Yeh T.J, Chen YJ, Hwang W..Y, Lin J.L. Incorporating fan control into air-conditioning systems to improve energy efficiency and transient response. Appl Therm Eng 2009;29:1955–64. https://doi.org/10.1016/J.APPLTHERMALENG.2008.09.017.
[42] Deymi-Dashtebayaz M, Farahnak M, Abadi R.N.B. Energy saving and environmental impact of optimizing the number of condenser fans in centrifugal chillers under partial load operation. International Journal of Refrigeration 2019;103:163–79. https://doi.org/10.1016/J.IJREFRIG.2019.03.020.
[43] IMST-Group Instituto de Ingeniería Energética Universidad Politécnica de Valencia. IMST-Art 2021.
[44] Blanco Castro J, Urchueguía J.F, Corberán J.M, Gonzálvez J. Optimized design of a heat exchanger for an air-to-water reversible heat pump working with propane (R290) as refrigerant: Modelling analysis and experimental observations. Appl Therm Eng 2005;25:2450–62. https://doi.org/10.1016/j.applthermaleng.2004.12.009.
[45] Pisano A, Martínez-Ballester S, Corberán J.M, Mauro A.W. Optimal design of a light commercial freezer through the analysis of the combined effects of capillary tube diameter and refrigerant charge on the performance. International Journal of Refrigeration 2015;52:1–10. https://doi.org/10.1016/j.ijrefrig.2014.12.023.
[46] Pitarch-Mocholi M, Navarro-Peris EE, Gonzalvez-Macia J, Corberan J.M. Comparative analysis of two subcritical heat pump boosters using subcooling in order to increase the efficiency of systems with a high water temperature glide. 12th IEA Heat Pump Conference, Rotterdam : 2017.
[47] Corberán J-M, Martínez-Galván I, Gonzálvez-Maciá J, Martínez-Ballester S. Influence of the source and sink temperatures on the optimal refrigerant charge of a water-to-water heat pump. IIR 1st Workshop on Refrigerant Charge Reduction, France: 2009.
[48] Air-Conditioning H and RI. AHRI 550/590 (I-P) and 551/591 (SI): Performance Rating of Water-Chilling and Heat Pump Water-Heating Packages Using the Vapor Compression Cycle 2020.
[49] Catrini P, Piacentino A. Experimental performance characterization of variable-speed packaged rooftop units with fouled evaporator. Appl Therm Eng 2023;233:121159. https://doi.org/10.1016/j.applthermaleng.2023.121159.
[50] Deru M, Field K, Studer D, Benne K, Griffith B, Torcellini P, et al. U.S. Department of Energy Commercial Reference Building Models of the National Building Stock. 2011.
[51] UNI. UNI/TR 11552:2014 "Opaque envelope components of buildings - Thermo-physical parameters. Available at: https://store.uni.com/uni-tr-11552-2014
[52] Klein SA. TRNSYS 17: A Transient System Simulation Program. Solar Energy Laboratory, University of Wisconsin, Madison, USA 2010.

[53] Meteonorm: Meteonorm, Global Meteorological Database. 2015:Handbook part II: theory, version 7.1.7.201517.